Article

Landsat Hourly Evapotranspiration Flux Assessment using Lysimeters for the Texas High Plains

Ahmed A. Hashem [1,2], Bernard A. Engel [3,*], Vincent F. Bralts [3], Gary W. Marek [4], Jerry E. Moorhead [4], Mohamed Rashad [2], Sherif Radwan [2] and Prasanna H. Gowda [5]

[1] College of Agriculture, Arkansas State University, 422 University Loop W, Jonesboro, AR 72401, USA; ahashem@astate.edu

[2] Agricultural Engineering Department, Suez Canal University, Ismailia 41522, Egypt; Abouzed1@yahoo.com (M.R.); Sherifradwa58@hotmail.com (S.R.)

[3] Agricultural & Biological Engineering Department, Purdue University, West Lafayette, IN 47907, USA; bralts@purdue.edu

[4] USDA-ARS Conservation and Production Research Laboratory, Bushland, TX 79012, USA; Gary.Marek@usda.gov (G.M.); jedmoorhead@yahoo.com (J.M.)

[5] USDA-ARS Southeast Area, Stoneville, MS 38776, USA; prasanna.gowda@usda.gov

* Correspondence: engelb@purdue.edu; Tel.: +1-765-494-8362

Abstract: Evapotranspiration (ET) is one of the biggest data gaps in water management due to limited ET measurements, and further, spatial variability in ET is difficult to capture. Satellite-based ET estimation has great potential for water resources planning as it allows estimation of agricultural water use at field, landscape, and watershed scales. However, uncertainties with satellite data derived ET are a major concern. This study evaluates hourly satellite-based ET from 2001–2010 for the growing season (May–October) under irrigated and dryland conditions for both tall and short crops. The evaluation was conducted using observed ET from four large weighing lysimeters at the United States Department of Agriculture Agricultural Research Service (USDA-ARS) Conservation and Production Research Laboratory in Bushland, Texas. Hourly ET from satellite data were derived using the Mapping Evapotranspiration at High Resolution with Internalized Calibration (METRIC) model. Performance statistics showed that satellite-based hourly estimates compared to lysimeter measurements provided good performance with an root-mean-square error $(RMSE)$ of 0.14 mm, Nash–Sutcliffe efficiency (NSE) of 0.57, and R^2 of 0.62 for ET for dryland crops, and $RMSE$ of 0.16, NSE of 0.63, and R^2 of 0.65 for irrigated crops. METRIC provided accurate hourly ET estimates that may be useful for irrigation scheduling and other water resources management purposes based on the hourly assessment.

Keywords: evapotranspiration; METRIC; remote sensing; irrigation water management; Landsat; lysimeter

1. Introduction

Evapotranspiration (ET) is one of the major components of the water budget. It plays a major role in the water cycle and irrigation water management [1,2]. Further, ET is the main consumer of rainfall and irrigation water in irrigated agricultural fields in arid and semiarid regions of the world. ET measurement methods such as pan evaporation, sap flow, and weighing lysimeters are widely used. These measurements are considered point estimates for particular irrigation practices in a homogenous field. Measuring ET on a watershed scale is challenging due to unavailability of direct measurement methods at that scale [3,4]. Other ET methods such as Bowen ratio, scintillometers, and eddy covariance can provide greater spatial coverage but may not adequately represent a watershed scale. Remote sensing models using satellite data can provide large-scale spatial coverage at various

spatial resolutions [5,6]. Considering the limitation that multiple weather parameters are required for ET modeling (air temperature, relative humidity, and wind speed), uncertainties also exist with satellite ET estimates [7].

Weighing lysimeters are considered the most accurate method for measurement for ET [8,9] as they directly measure the change in mass of a representative soil volume as ET occurs. Lysimeters vary in size, design, and weighing method but have shown applicability to a variety of crops, fruit trees, and forests [10]. Large weighing lysimeters can have sufficient depth and surface area as to not impede crop and root growth; however, shallower or smaller lysimeters may cause restrictions on plant development in addition to affecting drainage and soil water dynamics. These issues can cause discrepancies between the field surrounding the lysimeters or between different lysimeters. However, properly designed and maintained lysimeters can be managed in such a way that the conditions on the lysimeter are the same as the surrounding field, giving field-scale, directly measured ET data. These data still may not be representative of various land uses and management methods at a watershed scale; however, they can provide enough spatial resolution for validation of other ET measurements, such as remote sensing models.

Remote-sensing (RS)-based ET models are better suited than point estimates for estimating crop water use at a regional scale [11]. Numerous remote-sensing-based ET algorithms with varying complexities have been developed and are available for estimating the magnitude and trends in regional ET [12]. Daily, weekly, monthly, and seasonal ET estimation are the most dominant temporal resolutions using remote sensing for regional and watershed scales [13,14]. Gowda et al. [12] reported that daily ET estimates differed by 3% to 35% compared to ET measurements obtained using Bowen ratio and EC methods. Error sources include: (a) modeling errors and (b) measurement uncertainties and discrepancies in model-measurement scales, which are often not adequately accounted for in model testing studies. Errors are associated with all ET determination methods, but many can be minimized by increasing measurement accuracy and by careful quality assessment and quality control of ancillary data [12,15].

Accurate testing of field surface energy balance models, including those based on thermal imagery, depends on the ground truth and remotely sensed data accuracy. At watershed and basin scales, few examples of calibration of satellite-based ET using ground truth data measurements have occurred. These studies used ground truth from mass balance methods, including weighing lysimeters and the soil water balance, and EC measurements based on the energy balance to perform analysis on RS-based energy balance estimates of ET.

One of the major sources of ET estimation uncertainty using satellite energy balance models is the hourly satellite calibration [16,17]. This uncertainty can be minimized by comparing the hourly satellite estimates of evapotranspiration (ET), surface temperature (T_s), net solar radiation (R_n), and soil heat flux (G_o) to the measurements. This calibration is achieved for each image to reduce bias with radiometric accuracy related to the changing aerodynamics of the satellite scene, thermal conditions, and bias related to modeler estimates of the extreme conditions (dry and wet pixels). A dry pixel is described as bare agricultural soil, with high temperature and low evaporation rate, and a wet pixel is described as fully covered agricultural soil, with low temperature and high transpiration rate.

Hourly ET assessment has many benefits, including understanding sources of uncertainty with daily, weekly, monthly, seasonal, and yearly ET estimation. Accuracy assessment of hourly ET is a major step to quantify estimation errors with irrigation water management practices.

This study evaluated the hourly ET estimates of a 10-year period since the hourly estimates are the main component for various time scale ET interpolations. Previous studies evaluated daily, monthly, seasonal, and/or yearly ET estimates; however, no existing study has evaluated the hourly ET for irrigation management purposes. Evaluating hourly ET estimates is crucial to quantify uncertainties associated with the daily, monthly, seasonal, and yearly estimates for irrigation management purposes.

2. Materials and Methods

2.1. Site Description

Four fields equipped with lysimeters at the USDA-ARS Conservation and Production Research Laboratory at Bushland, TX (35.19° N, 102.10° W) at an elevation of 1170 m above mean sea level were selected for this study. The research field is a square with a surface area of approximately 20 ha, subdivided into four quadrants of approximately 4.7 ha each. A precision, large weighing lysimeter is located at the center of each quadrant; two lysimeters were managed as dryland (NW and SW), and the other two lysimeters were managed as irrigated (NE and SE) during the study years. The observed data were combined for each lysimeter, and statistical performance assessment was performed for the estimated values for each parameter for the two dryland lysimeters (NW and SW) and the two irrigated lysimeters (NE and SE). The soil characteristics for the study field are deep, well-drained Pullman silty clay loam (fine, mixed, superactive, thermic Torrertic Paleustoll) [18]. The local climate is classified as semi-arid, with large daily temperature variations. Cotton, soybean, grain and silage sorghum, sunflower, and cotton were the predominant crops for the research fields.

2.2. Weather Parameter Measurements

Dataloggers (CR6, Campbell Scientific, Logan, Utah) were used to collect data using the following sensors: air temperature and relative humidity sensor (HMP155, Vaisala, Helsinki, Finland), four soil water sensors (Acclima 315, Acclima Inc., Meridian, Idaho), six soil heat flux plates (HFT-3, Radiation Energy Balance Systems, Bellevue, Washington), an infrared thermometer, and a net radiometer (Q*7.1, Radiation Energy Balance Systems, Bellevue, Washington) [19]. These sensors were utilized to measure surface temperature, soil heat flux, and net solar radiation over each lysimeter. The QA/QC protocol from Evett et al. [20] was performed on the collected data. Weather parameter data were recorded every 6 s and summed or averaged for 30-min intervals.

The solar radiation sensor calibration was performed to assess the sensor accuracy through evaluating the observed R_n with the sum of measured downwelling and upwelling short- and longwave radiation as well as comparing to the theoretical maximum clear sky solar irradiance. Based on the sensor calibration results, the sensor performance was accurate in solar radiation measurement.

Colaizzi et al. [21] highlighted the soil heat flux calculation and calibration process for 30-min time intervals. The calibration process was performed using the soil water and temperature sensor data to calculate the change in soil heat storage from the surface to the soil heat flux plates.

2.3. Landsat Imagery

Landsat Collection-1 was used for Landsat 5 Thematic Mapper (TM) satellite data throughout the growing season (May–October). The images were obtained through Earth Explorer (https://earthexplorer.usgs.gov/), with two satellite paths (30 and 31) and row 36 from 2001 to 2010. A total of 53 cloud-free images were acquired, as the presence of clouds can cause errors in the estimation process due to aerodynamics and radiometric disturbance [17]. Appendix A includes day of year (DOY) for images used. The Landsat 5 TM consists of six spectral bands (bands 1–5 and band 7) with spatial resolutions of 30 m and one thermal band (band 6) with a spatial resolution of 120 m. Top-of-atmosphere reflectance was used to calculate NDVI Equation (5) using the red and near-infrared bands [22].

2.4. Image Analysis

The Bushland Evapotranspiration and Agricultural Remote Sensing (BEARS) software is an image processing and geographic information system software deriving hourly, daily, and seasonal evapotranspiration maps. It also produces other energy exchange outputs between land and atmosphere using Landsat 5, 7, and 8 [23]. The BEARS software was used for this analysis to estimate the hourly *ET*, T_s, R_n, and G_o for the four lysimeters. The BEARS software is public domain software

that offers users the option to select one of five energy-balance-based ET methods: Mapping Evapotranspiration at High Resolution with Internalized Calibration (METRIC), Surface Energy Balance Algorithm for Land (SEBAL), Surface Energy Balance System (SEBS), Tow Source Model (TSM), and Simplified Surface Energy Balance (SSEB). The METRIC model has been utilized in this study. To extract the average value of each parameter, a grid of 3 by 3 pixels was selected, with each lysimeter located towards the center of this grid.

The Mapping Evapotranspiration at High Resolution with Internalized Calibration (METRIC) model is a satellite image processing model that is used for ET estimation as a residual of the energy balance for various short crops, tall crops, trees, and forest [24–32] Equation (1).

$$E = R_n - G - H \tag{1}$$

where LE is the latent heat flux density [W m⁻²], R_n is the net radiation [W m⁻²], G is the soil heat flux [W m⁻²], and H is the sensible heat flux density [W m⁻²].

METRIC has been employed for Landsat image analysis (with a spatial resolution of 30 m) for agricultural water use and other agricultural applications that require field-scale resolution. The energy balance is evaluated internally under two extreme conditions (dry and wet) using surface temperature, vegetation growth, and available weather data. The accuracy of ET estimation depends on user experience, and the estimation accuracy was found to be inversely related with ET levels, where low ET levels had high uncertainty and vice versa [33]. Those two extremes are the strength of METRIC, compared to the Surface Energy Balance System (SEBS) and other satellite-based ET models [25]. An automated statistical calibration method has been developed to better estimate the dry and wet pixels, enhancing ET estimation accuracy [17].

Atmospheric correction is not required for surface temperature (Ts) and reflectance (albedo) measurements using radiative transfer models due to the use of the indexed temperature gradient dT and the internal calibration of the sensible heat computation within METRIC [34]. Another advantage of using the internal calibration is that it reduces the bias with aerodynamic stability corrections and surface roughness.

Net radiation at the surface (R_n) is calculated by subtracting all outgoing radiant fluxes from all incoming radiant fluxes including solar and thermal radiation Equation (2):

$$R_n = R_{S\downarrow} - \alpha R_{S\downarrow} + R_{L\downarrow} - R_{L\uparrow} - (1 - \varepsilon_o)R_{L\downarrow} \tag{2}$$

where $R_{S\downarrow}$ is the incoming short-wave radiation [W m⁻²], α is the surface albedo (dimensionless), $R_{L\downarrow}$ is the incoming long-wave radiation [W m⁻²], $R_{L\uparrow}$ is the outgoing long-wave radiation [W m⁻²], ε_o is the broad-band surface thermal emissivity (dimensionless), and $(1 - \varepsilon_o)R_{L\downarrow}$ is the fraction of incoming long-wave radiation reflected from the surface.

The surface temperature (T_s) is calculated for Landsat images using the modified Planck equation, based on Markham [35], with both atmospheric and surface emissivity correction, as shown in Equation (3).

$$T_s = \frac{K_2}{\ln\left[\left(\varepsilon_{NB} K_1/R_c\right)+1\right]} \tag{3}$$

where $K_1 \ and \ K_2$ are constants ($K_1 = 607.8 \ and \ K_2 = 1261$ [W m⁻² sr⁻¹ μm⁻¹]for Landsat 5), ε_{NB} is the narrow-band emissivity corresponding to satellite thermal sensor wavelength band, and R_c is the corrected thermal radiance from the surface using spectral radiance $L_{t,thermal}$ from the thermal band of Landsat.

The corrected thermal radiance (R_c) [W m⁻² sr⁻¹ μm⁻¹] is calculated using Equation (4) [36]:

$$R_c = \frac{L_{t,thermal} - R_P}{T_{NB}} - (1 - \varepsilon_{NB})R_{sky} \tag{4}$$

where $L_{t,thermal}$ is the spectral radiance of Landsat 5 thermal band [W m⁻² sr⁻¹ μm⁻¹], R_P is the path radiance in the 10.4–12.5 μm band [W m⁻² sr⁻¹ μm⁻¹], T_{NB} is the narrow-band emissivity of air (10.4–12.5 μm range), and R_{sky} is the narrow-band downward thermal radiation from a clear sky [W m⁻² sr⁻¹ μm⁻¹].

The normalized difference vegetation index (*NDVI*) is the ratio of the differences in reflectivity for the near-infrared band and the red band divided by the sum Equation (5).

$$NDVI = \frac{(\rho_{t,nir} - \rho_{t,red})}{(\rho_{t,nir} + \rho_{t,red})} \tag{5}$$

where $\rho_{t,nir}$ is the reflectance of the near-infrared band, and $\rho_{t,red}$ is the reflectance of the red band.

The soil heat flux represents the rate of heat storage in the soil and vegetation as a result of conduction. METRIC calculates G as a ratio $\frac{G}{R_n}$ using Equation (6) [37] to represent values near mid-day.

$$\frac{G}{R_n} = (T_s - 273.15)(0.0038 + 0.0074\alpha)(1 - 0.98\,NDVI^4) \tag{6}$$

where T_s is the surface temperature (K), and α is the surface albedo.

Alternatively, [38] developed the ratio $\frac{G}{R_n}$ using soil heat flux data collected by USDA-ARS [39] for an irrigated crop near Kimberly, Idaho, as represented in Equations (7) and (8).

$$\frac{G}{R_n} = 0.05 + 0.18\,e^{-0.521\,LAI} \qquad (LAI \geq 0.5) \tag{7}$$

$$\frac{G}{R_n} = 1.80\,{}^{(T_s - 273.15)}/_{R_n} + 0.084 \qquad (LAI < 0.5) \tag{8}$$

where LAI is the leaf area index, and T_s is the surface temperature.

METRIC sensible heat flux calculation is estimated from the aerodynamic function as listed in Equation (9).

$$H = \rho_{air}\,C_P\,\frac{dT}{r_{ah}} \tag{9}$$

where ρ_{air} is the air density [kg m^{-3}], C_P is the specific heat of air at constant pressure [J kg^{-1}K^{-1}], r_{ah} is the aerodynamic resistance [s m^{-1}] between two near-surface heights, $z_1\,and\,z_2$ (always 0.1 and 2 m) computed in a particular pixel, and dT is the near-surface temperature difference (K) between $z_1\,and\,z_2$.

In METRIC, the r_{ah} calculation uses wind speed extrapolation from blending heights (normally 100 to 200 m) above the ground surface. dT is used in Equation (9) due to complications in estimating surface temperature accurately from satellites, which arise from uncertainties in atmospheric attenuation or contamination and radiometric calibration of the sensor [25]. The surface temperature obtained by the satellite, whether it is a radiometric or kinematic temperature, can also be different by several degrees from the aerodynamic temperature, the main driver for the heat transfer process [3,40,41]. dT can be estimated using Equation (10) [42].

$$dT = a + bT_{s\,datum} \tag{10}$$

Where $a\,and\,b$ are the empirical constants for a given Landsat satellite image, and $T_{s\,datum}$ is the surface temperature adjusted to a common elevation for each image pixel using a digital elevation model and customized lapse rate.

Determining accurate hot (dry) and cold (wet) pixels is one of the most critical and challenging steps in implementing METRIC to spatially estimate ET [17,33]. A manual selection method was performed to determine the dry and wet pixels using the surface temperature and the NDVI outputs based on the criteria listed in Table 1. The manual selection process was performed using the surface temperature (T_s) and NDVI histogram distribution. Obtaining the T_s distribution is necessary to determine the range of the high and low temperature threshold for each image.

Table 1. Hot and cold pixel description and constraint limits.

Parameter	Condition	Constraint		Outcome
		T_s	NDVI	
Lowest ET	Bare agricultural soil	High	≤ 0.2	Hot pixel location (x,y)
Highest ET	Cultivated agricultural soil	Low	≥ 0.7	Cold pixel location (x,y)

Several iterations were implemented to obtain the most accurate hot and cold pixels that met the conditions listed in Table 1. The more accurate the dry and wet pixel determination, the better the ET estimates across the satellite scene. Special consideration of the hot and cold pixel selection, such as avoiding the image edges, as well as the hot and cold pixels distribution across the scene instead of centralizing the pixels toward a specific location was used.

2.5. Statistical Analysis

In addition to visual inspection of observed and simulated ET values for pixels covering lysimeters, the satellite-based ET performance was evaluated for the selected day's images that were available. Various statistical parameters were estimated, including Nash–Sutcliffe efficiency (*NSE*), root-mean-square error (*RMSE*), and mean bias error (*MBE*), to evaluate the relationship strength between simulated and measured values [19,43,44]. *RMSE* and *MBE* were calculated using Equations (11) and (12), respectively. Linear regression was performed to determine the coefficient of determination (R^2), the slope and intercept, and Nash–Sutcliffe efficiency (*NSE*; Nash and Sutcliffe, 1970) (Equation (13) [45]. The slope of 1.0, intercept of zero, and R^2 approaching 1.0 indicates a perfect fit. The *MBE* provides the ability to determine the deviation between the measured and satellite-based estimates, with *MBE* = 0 indicating no bias in estimation. The *NSE* values can range from -∞ to +1, with +1 being a perfect agreement between the model and observed data [46].

$$MSE = \sqrt{\frac{\sum_{i=1}^{n}(\hat{y}_t - y_t)^2}{n}} \tag{11}$$

$$MBE = \frac{\sum_{i=1}^{n}(y_t - \hat{y}_t)}{n} \tag{12}$$

where y_t = the *i*-th observed value, $\hat{y}_t$ = the *i*-th simulated value, and n = total number of observations.

$$NSE = 1 - \frac{\sum_i (y_m - y_s)_i^2}{\sum_i (y_{m,j} - \bar{y}_m)^2} \tag{13}$$

where $\bar{y}_m$ is the average measured value, $\bar{y}_s$ is the average simulated value, y_m is the measured data on day i, y_s is the simulated output on day *i*, and j represents the rank.

3. Results

3.1. Lysimeter Comparison

The METRIC model [25] was used to estimate ET, and an hourly evaluation was performed for surface temperature, solar radiation, soil heat flux, and evapotranspiration (T_s, R_n, G_o, ET). The evaluation process was conducted for tall crops, including forage sorghum and forage corn; short crops including cotton, sunflowers, and soybeans; and bare soil for the dryland and irrigated lysimeters.

Tables 2 and 3 summarize the statistical performance of the METRIC model estimation for T_s, R_n, G_o, and ET versus the observed lysimetric data. The regression line between the observed and simulated values for the dryland and irrigated lysimeters can be found in Figures 1 and 2, respectively.

The observed mean hourly surface temperature value for the dryland lysimeter at the time of satellite overpass was 33.8 °C, and it closely matched the estimated mean value of 33.0 °C. The dryland lysimeter regression line for surface temperature had a good coefficient of determination of 0.76, with a slope and intercept of 0.7 and 9.3 °C. The *RMSE* was ~6.8% (2.3 °C of the mean observed values, with an *MBE* of 0.8 °C.

Figures 1b and 2b represent the R_n comparison between dryland and irrigated lysimeters, respectively, compared to the measured data. The dryland model estimated R_n value was 521.5 W M^{-2}, and it closely matched the measured value of 533.5 W M^{-2}. The irrigated lysimeter estimate was 551.3 W M^{-2}, and the observed R_n was 542.3 W M^{-2}. The dryland lysimeter model provided good performance for net radiation with an NSE of 0.68 and poor performance for the irrigated lysimeter with an *NSE* of 0.17. The regression model for dryland lysimeters accounted for 71% of the variability, with a slope of 0.8 and intercept of 98.2 W M^{-2} (Table 2). The irrigated regression model captured 22% of the variability, which is lower than for the dryland regression model, with a slope of 0.29 and intercept of 392.3 W M^{-2} (Table 3).

Figures 1d and 2d represent the soil heat flux comparison between dryland and irrigated lysimeters and satellite estimates. Both irrigated and dryland conditions underestimated the soil heat flux compared to the observed values. Consequently, the summary statistics provided a weak correlation for irrigated and dryland lysimeter soil heat flux. The METRIC mean estimated G_o for dryland was 34.5 W M^{-2} and the observed was 38.6 W M^{-2}, with 10.6% underestimation for the dryland condition. The irrigated lysimeter mean estimated value was 35.6 W M^{-2}, and the observed value was 38.6 W M^{-2}, with 2.2% underestimation for the irrigated lysimeter.

The mean hourly estimated ET for dryland was 0.33 mm h^{-1}, and the mean observed *ET* was 0.28 mm h^{-1}. For the irrigated model, the mean simulated value was 0.47 mm h^{-1}, and the mean observed value was 0.43 mm h^{-1}.
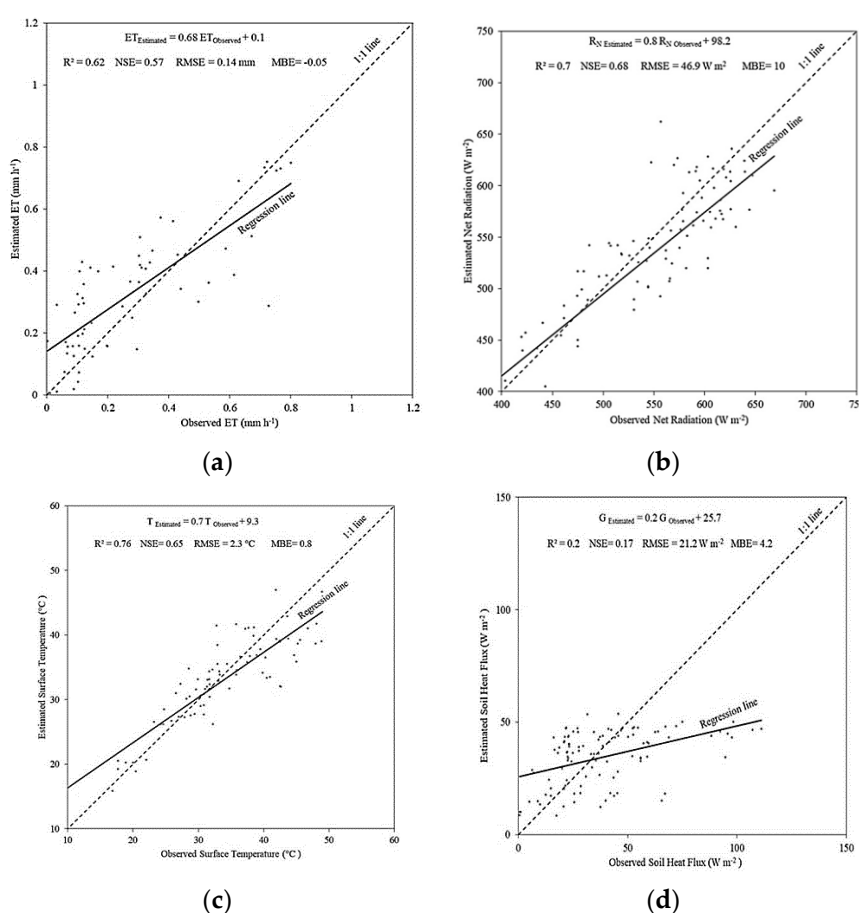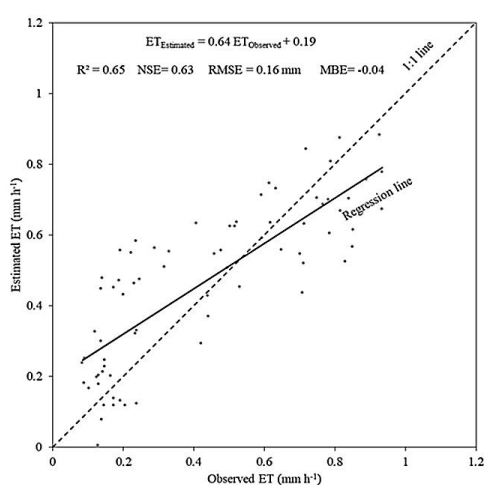

Figure 1. Regression relationship between observed hourly evapotranspiration (**a**), net radiation (**b**), surface temperature (**c**), and soil heat flux (**d**) from 2001–2010 for NW and SW dryland lysimeters.

Table 2. Performance statistics of surface energy balance components using Mapping Evapotranspiration at High Resolution with Internalized Calibration (METRI)C for dryland lysimeters (NW and SW) from 2001–2010.

Estimated parameter	Mean		*RMSE*	*MBE*	*NSE*	Regression	
	Observed	Estimated				R^2	*Slope*
T (℃)	33.8	33.0	2.3	0.8	0.65	0.76	0.70
R_n (W m^{-2})	533.5	521.5	46.9	10.0	0.68	0.71	0.80
G_o (W m^{-2})	38.6	34.5	21.2	4.2	0.17	0.20	0.20
ET (mm h^{-1})	0.28	0.33	0.14	−0.05	0.57	0.62	0.68

Table 3. Performance statistics of surface energy balance components using METRIC for irrigated lysimeters (NE and SE) from 2001–2010.

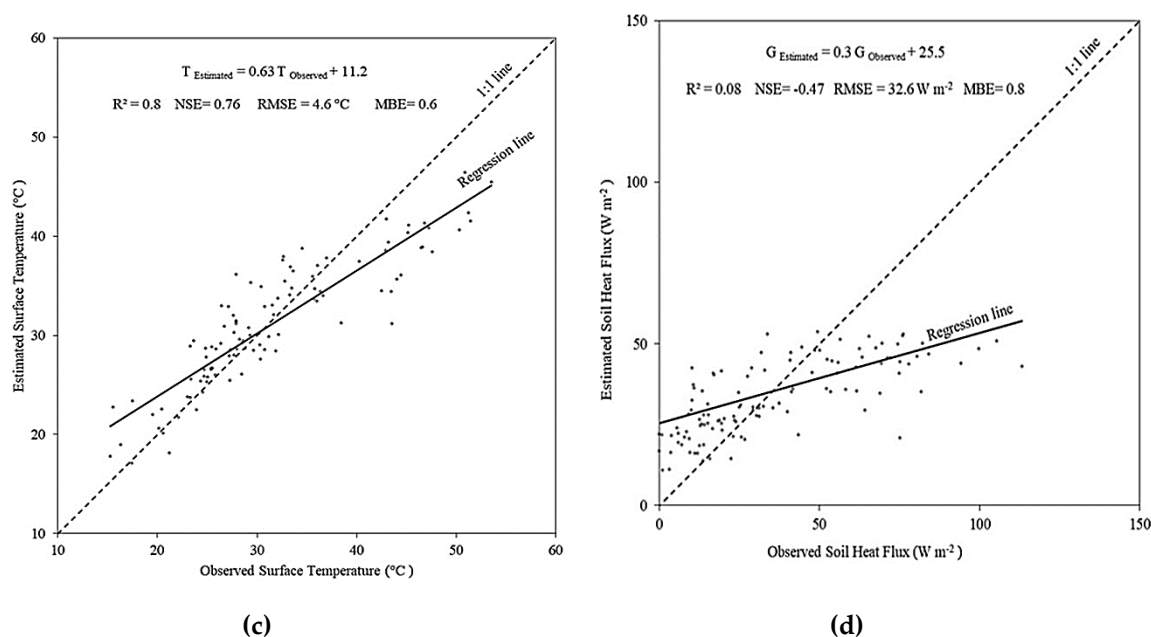| Estimated parameter	Mean		*RMSE*	*MBE*	*NSE*	Regression	
	Observed	Estimated				R^2	*Slope*
T (℃)	31.5	31.2	4.6	0.55	0.76	0.80	0.63
R_n (W m^{-2})	542.3	551.3	84.8	−9.0	0.17	0.22	0.29
G_o (W m^{-2})	36.4	35.6	32.6	0.8	−0.47	0.08	0.30
ET (mm h^{-1})	0.43	0.47	0.16	−0.04	0.63	0.65	0.64

(a)
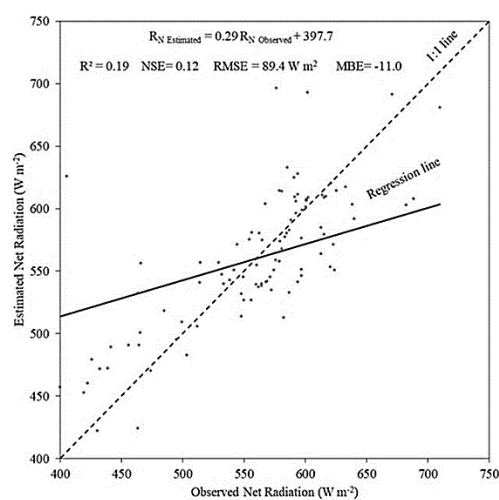
(b)

Figure 2. Regression relationship between observed hourly evapotranspiration (**a**), net radiation (**b**), surface temperature (**c**), and soil heat flux (**d**) from 2001–2010 for NE and SE irrigated lysimeters.

4. Discussion

The hourly comparison for the lysimeter site was performed for surface temperature, evapotranspiration, net radiation, and soil heat flux. The observed surface temperature for the dryland lysimeter was higher than the irrigated lysimeter (Figures 1c and 2c), as expected. The hourly evaluation of the METRIC model illustrated good performance for both water management conditions; however, the irrigated lysimeter overall hourly comparison provided slightly better statistics than the dryland lysimeter. The dryland lysimeter observed and estimated temperatures are higher than for the irrigated lysimeter, and this is due to the irrigation cooling effect.

The observed mean surface temperature value for the irrigated lysimeter was 31.5 °C, and it closely matches the estimated mean value of 31.2 °C. The irrigated lysimeter regression line for surface temperature has better estimates than for the dryland lysimeter, with a coefficient of determination of 0.8, a slope and an intercept of 0.63 and 11.2 °C. The *RMSE* was 14.6% (4.6 °C) of the mean observed values with *MBE* of 0.55 °C. These predicted errors are close to those reported in the literature [43,47–50]. Moorhead and Gowda have similar unpublished reports for METRIC hourly comparisons. The *NSE* values of 0.65 and 0.76 for the dryland and irrigated surface temperatures, respectively, are viewed as a good match [27,31,43].

The *RMSE* for the solar radiation for dryland lysimeters was lower than for irrigated lysimeters, with values of 8.8% (46.9 W M^{-2}) and 15.6% (84.8 W M^{-2}), for the dryland and irrigated lysimeters, respectively. These errors may have resulted from estimation errors in air emissivity and surface albedo as well as the water content in the air above the irrigated field being higher compared to the dryland lysimeter. This water content may distort the electromagnetic reflectance more than for dry fields, resulting in poor solar radiation estimates. These errors ranged within reported values in the literature [31,43,51–54].

As a result of soil heat flux underestimation, the *NSE* values were 0.17 and –0.47 for dryland and irrigated lysimeters, respectively, which indicated poor performance for the irrigated field compared to the dryland lysimeter. The *RMSE* and *MBE* for the dryland were 55% (21.2 W M^{-2}) and 4.2 W M^{-2}, respectively; the *RMSE* and *MBE* for the irrigated lysimeter were 89.6 and 0.8 W M^{-2}, respectively. The dryland regression model accounted for 20% of the variability in measured data with a slope of 0.2 and intercept of 25.7 W M^{-2} (Table 2). The irrigated regression model accounted for only 8% of variability, with a slope of 0.3 and intercept of 25.5 W M^{-2} (Table 3). The range of satellite-estimated soil heat fluxes is much lower than that with the observed data, indicating

METRIC is underestimating soil heat flux, possibly due to the time difference between the physical process of conduction and the instantaneous acquisition of the satellite image. The wet conditions of the irrigated fields may have an impact on the estimation accuracy of R_n and G_0 due to the humidity above the soil surface. Accuracy in the estimation of R_n and G_0 may be affected by increased humidity near the top of the canopy on the irrigated lysimeter, which may disturb the electromagnetic radiation reflectance compared to the dryland lysimeter. These results agree with [27,31,43].

The METRIC *ET* estimation provided a good correlation for the dryland model; however, METRIC *ET* estimation performed better for the irrigated conditions. The hourly *ET* regression model explained 62% of the *ET* variability in the observed data for dryland lysimeters, with a slope of 0.68 and an intercept of 0.1 mm h^{-1}. The regression model for irrigated conditions estimated 65% of the variation in the observed data, with a slope of 0.64 and an intercept of 0.19 mm h^{-1}.

The dryland *RMSE* for the hourly *ET* was 0.14 mm, which was 50% higher than that of the mean observed *ET*; the *MBE* was −0.05 mm. The irrigated modeled hourly *ET RMSE* was 0.16 mm h^{-1}, about 37.2% higher than that of the mean observed hourly ET; the *MBE* was −0.04 mm. The irrigated lysimeters error values were less than those of the dryland lysimeter (Tables 2 and 3), possibly due to increased overall *ET* and less sensible heat flux, which may have caused attenuation in the reflected radiation from the dryland field as captured by the satellite. Overall, these results agreed with [23,45], illustrating that the accuracy level of METRIC hourly T_s, R_n, and G_0 for dryland and T_s and R_n for irrigated lysimeter estimation are considered good for the Texas High Plains, with potential applications for other geographic locations. These results are within the range reported in the literature [12,27,29–31,44,54–56].

5. Conclusions

The METRIC model was tested against lysimetric hourly surface temperature (T_s), net radiation (R_n), soil heat flux (G_0), and evapotranspiration (*ET*) in the Texas High Plains. For this purpose, 53 cloud-free images from Landsat 5 TM acquired during 2001–2010 were used. The hourly values were extracted and compared against observed T_s, R_n, G_0, and *ET* for different (tall and short) crops as well as bare soil conditions managed under dryland and irrigated conditions. The METRIC model performance was good in estimating T_s, R_n, and *ET* under dryland conditions and T_s and *ET* for irrigated conditions. The wet conditions in the irrigated lysimeter fields affected electromagnetic reflectance.

The overall accuracy level of the Landsat estimates of the evaluated parameters (surface temperature, net radiation, soil heat flux, and evapotranspiration) indicate that the METRIC model may be suitable for deriving hourly input at a watershed scale with fairly good accuracy.

Supplementary Materials: The following are available online at www.mdpi.com/2073-4441/12/4/1192/s1, Table S1: USDA-ARS Bushland, Texas site Landsat images dates and corresponding Day of Year (DOY).

Author Contributions: Writing—original draft A.A.H.; methodology, A.A.H. and P.H.G.; software, J.E.M. and P.H.G.; formal analysis, M.R. and S.R.; resources, P.H.G.; review and editing, B.A.E., V.F.B., and J.E.M.; supervision, B.A.E. All authors have read and agreed to the published version of the manuscript.

Conflicts of Interest: The authors declare no conflict of interest.

References

1. Sentelhas, P.C.; Gillespie, T.J.; Santos, E.A. Evaluation of FAO Penman-Monteith and alternative methods for estimating reference evapotranspiration with missing data in Southern Ontario, Canada. *Agric. Water Manag.* **2010**, *97*, 635–644.

2. Gavilán, V.; Lillo-Saavedra, M.; Holzapfel, E.; Rivera, D.; García-Pedrero, A. Seasonal Crop Water Balance Using Harmonized Landsat-8 and Sentinel-2 Time Series Data. *Water* **2019**, *11*, 22–36.

3. Qualls, R.J.; Brutsaert, W. Effect of Vegetation Density on the Parameterization of Scalar Roughness to Estimate Spatially Distributed Sensible Heat Fluxes. *Water Resour. Res.* **1996**, *32*, 645–652.

4. Ayyad, S.; Al Zayed, I.S.; Ha, V.T.T.; Ribbe, L. The Performance of Satellite-Based Actual Evapotranspiration Products and the Assessment of Irrigation Efficiency in Egypt. *Water* **2019**, *11*, 1913.

5. PÔças, I.; Paço, T.A.; Cunha, M.; Andrade, J.A.; Silvestre, J.; Sousa, A.; Santos, F.L.; Pereira, L.S.; Allen, R.G. Satellite-based evapotranspiration of a super-intensive olive orchard: Application of METRIC algorithms. *Biosyst. Eng.* **2014**, *128*, 69–81.

6. Torres-Rua, A.; Ticlavilca, A.; Bachour, R.; McKee, M. Estimation of Surface Soil Moisture in Irrigated Lands by Assimilation of Landsat Vegetation Indices, Surface Energy Balance Products, and Relevance Vector Machines. *Water* **2016**, *8*, 167.

7. Idso, S.B.; Jackson, R.D.; Reginato, R.J. Estimating evaporation: a technique adaptable to remote sensing. *Science* **1975**, *189*, 991–2.

8. Evett, S.; Schwartz, R.; Howell, T.A.; Baumhardt, R.L.; Copeland, K.S. Can weighing lysimeter ET represent surrounding field ET well enough to test flux station measurements of daily and sub-daily ET? *Adv. Water Resour.* **2012**, *50*, 79–90.

9. Howell, T.A.; Schneider, A.D.; Jensen, M.E. History of lysimeter design and use for evaportanspiration measurements. In *Lysimeters for Evapotranspiration and Environmental Measurements*, In Proceedings of the International Symposium on Lysimetry; Honolulu, HI, USA, 23–25 July, 1991.

10. Allen, R.; Fisher, D.K. Direct load cell-based weighing lysimeter system. In *Lysimeters for Evapotranspiration and Environmental Measurements*, In Proceedings of the International Symposium on Lysimetry, Honolulu, HI, USA, 23–25 July, 1991.

11. Allen, R.G.; Tasumi, M.; Morse, A.; Trezza, R.; Wright, J.L.; Bastiaanssen, W.; Kramber, W.; Lorite, I.; Robison, C.W. Satellite-Based Energy Balance for Mapping Evapotranspiration with Internalized Calibration (METRIC)—Applications. *J. Irrig. Drain. Eng.* **2007**, *133*, 395–406.

12. Gowda, P.H.; Chavez, J.L.; Colaizzi, P.D.; Evett, S.R.; Howell, T.A.; Tolk, J.A. ET mapping for agricultural water management: present status and challenges. *Irrig. Sci.* **2008**, *26*, 223–237.

13. Senay, G.B.; Schauer, M.; Velpuri, N.M.; Singh, R.K.; Kagone, S.; Friedrichs, M.; Litvak, M.E.; Douglas-Mankin, K.R. Long-Term (1986–2015) Crop Water Use Characterization over the Upper Rio Grande Basin of United States and Mexico Using Landsat-Based Evapotranspiration. *Remote Sens.* **2019**, *11*, 1587.

14. Senay, G.B.; Bohms, S.; Singh, R.K.; Gowda, P.H.; Velpuri, N.M.; Alemu, H.; Verdin, J.P. Operational Evapotranspiration Mapping Using Remote Sensing and Weather Datasets: A New Parameterization for the SSEB Approach. *JAWRA J. Am. Water Resour. Assoc.* **2013**, *49*, 577–591.

15. Allen, R.G.; Pereira, L.S.; Howell, T.A.; Jensen, M.E. Evapotranspiration information reporting: I. Factors governing measurement accuracy. *Agric. Water Manag.* 2011, *98*, 899–920.

16. Allen, R.G.; Pereira, L.S.; Howell, T.A.; Jensen, M.E. Evapotranspiration information reporting: II. Recommended documentation. *Agric. Water Manag.* 2011, *98*, 921–929.

17. Allen, R.G.; Burnett, B.; Kramber, W.; Huntington, J.; Kjaersgaard, J.; Kilic, A.; Kelly, C.; Trezza, R. Automated Calibration of the METRIC-Landsat Evapotranspiration Process. 2013, *49*, 563–576.

18. Unger, P.W.; Pringle, F.B. *Pullman Soils: Distribution Importance, Variability, and Management*; Texas Agricultural Experiment Station: College Station, TX, USA, 1981.

19. Moorhead, J.E.; Marek, G.W.; Gowda, P.H.; Lin, X.; Colaizzi, P.D.; Evett, S.R.; Kutikoff, S. Evaluation of Evapotranspiration from Eddy Covariance Using Large Weighing Lysimeters. *Agronomy* **2019**, *9*, 99.

20. Evett, S.R.; Marek, G.W.; Copeland, K.S.; Colaizzi, P.D. Quality Management for Research Weather Data: USDA-ARS, Bushland, TX. *Agrosystems, Geosci. Environ.* **2018**, *1*. doi:10.2134/age2018.09.0036.

21. Colaizzi, P.D.; Evett, S.R.; Agam, N.; Schwartz, R.C.; Kustas, W.P.; Cosh, M.H.; McKee, L. Soil heat flux calculation for sunlit and shaded surfaces under row crops: 2. Model test. *Agric. For. Meteorol.* **2016**, *216*, 115–128.

22. Senay, G.B.; Friedrichs, M.; Singh, R.K.; Velpuri, N.M. Evaluating Landsat 8 evapotranspiration for water use mapping in the Colorado River Basin. *Remote Sens. Environ.* **2016**, *185*, 171–185.

23. Evett, S.R.; Kustas, W.P.; Gowda, P.H.; Anderson, C.A.; Prueger, J.H.; Howell, T.A. Overview of the Bushland Evapotranspiration and Agricultural Remote sensing EXperiment 2008 (BEAREX08): A field experiment evaluating methods for quantifying ET at multiple scales. *Elsevier* **2012**, *50*, 4–19.

24. Allen, R.; Morse, A.; Tasumi, M.; Trezza, R.; Bastiaanssen, W.; Wright, J.L.; Kramber, W. Evapotranspiration from a satellite-based surface energy balance for the Snake Plain Aquifer in Idaho. In Proceedings of the USCID Conference; San Luis Obispo, CA, USA, 9–12 July, 2002.

25. Allen, R.G.; Tasumi, M.; Trezza, R.; Morse, A.; Trezza, R.; Wright, J.L.; Bastiaanssen, W.; Kramber, W.; Lorite, I.; Robison, C.W. Satellite-Based Energy Balance for Mapping Evapotranspiration with Internalized Calibration (METRIC)—Model. *J. Irrig. Drain. Eng.* **2007**, *133*, 380–394.

26. Tasumi, M.; Trezza, R.; Allen, R.G.R.; Wright, J.L.J. Operational aspects of satellite-based energy balance models for irrigated crops in the semi-arid U.S. *Irrig. Drain. Syst.* **2005**, *19*, 355–376.

27. Hashem, A.A. Irrigation Water Management Using Remote Sensing and Hydrologic Modeling, Ph.D. Dissertation, Purdue University,West Lafayette, IN, USA, 2018.

28. Gowda, P.H.; Terry, A.H.; Jose, L.C.; George, P.; Moorhead, J.E.; Daniel, H.; Marek, T.H.; Porter, D.O.; Marek, G.H.; Colaizzi, P.D.; et al. *A Decade of Remote Sensing and Evapotranspiration Research at USDA-ARS Conservation and Production Research Laboratory*; American Society of Agricultural and Biological Engineers: St. Joseph, MI, USA, 2015; pp. 1–14.

29. Santos, C.; Lorite, I.J.; Allen, R.G.; Tasumi, M. Aerodynamic Parameterization of the Satellite-Based Energy Balance (METRIC) Model for ET Estimation in Rainfed Olive Orchards of Andalusia, Spain. *Water Resour. Manag.* **2012**, *26*, 3267–3283.

30. Numata, I.; Khand, K.; Kjaersgaard, J.; Cochrane, M.; Silva, S. Evaluation of Landsat-Based METRIC Modeling to Provide High-Spatial Resolution Evapotranspiration Estimates for Amazonian Forests. *Remote Sens.* **2017**, *9*, 46.

31. Rangaswamy, M.; A.; Khalid, A.-G.; Elkamil, T.; Hassaballa, A., A.; Patil, C.V. Performance of the METRIC model in estimating evapotranspiration fluxes over an irrigated field in Saudi Arabia using Landsat-8 images. *Hydrol. Earth Syst. Sci.* **2017**, *21*, 6135–6151.

32. El Ghandour, F.-E.; Alfieri, S.M.; Houali, Y.; Habib, A.; Akdim, N.; Labbassi, K.; Menenti, M. Detecting the Response of Irrigation Water Management to Climate by Remote Sensing Monitoring of Evapotranspiration. *Water* **2019**, *11*, 2045.

33. Morton, C.G.; Huntington, J.L.; Pohll, G.M.; Allen, R.G.; McGwire, K.C.; Bassett, S.D. Assessing Calibration Uncertainty and Automation for Estimating Evapotranspiration from Agricultural Areas Using METRIC. *J. Am. Water Resour. Assoc.* **2013**, *49*, 549–562.

34. Tasumi, M.; Allen, R.G.; Trezza, R.; Wright, J.L. Satellite-Based Energy Balance to Assess Within-Population Variance of Crop Coefficient Curves. *J. Irrig. Drain. Eng.* **2005**, *131*, 94–109.

35. Markham, L.B. Landsat MSS and TM post-calibration dynamic ranges, exoatmospheric reflectances and at-satellite temperatures. *Landsat Tech. Notes* **1986**, *1*, 3–8.

36. Wukelic, G.E.G.E.; Gibbons, D.E.; Martucci, L.M.M.; Foote, H.P.P. Radiometric calibration of Landsat Thematic Mapper thermal band. *Remote Sens. Environ.* **1989**, *28*, 339–347.

37. Bastiaanssen, W.G.M.; Molden, D.J.; Makin, I.W. Remote sensing for irrigated agriculture: Examples from research and possible applications. *Agric. Water Manag.* **2000**, *46*, 137–155.

38. Tasumi, M. Progress in Operational Estimation of Regional Evapotranspiration Using Satellite Imagery, Ph.D. Thesis, University of Idaho, Moscow, 2003.

39. Wright, J.L. New evapotranspiration crop coefficients. *Proc. Am. Soc. Civ.* **1982**, *108*, 57–74.

40. Kustas, W.P.; Moran, M.S.; Humes, K.S.; Stannard, D.I.; Pinter, J..; Hipps, L.E.; Swiatek, E.; Goodrich, D.C. Surface energy balance estimates at local and regional scales using optical remote sensing from an aircraft platform and atmospheric data collected over semiarid rangelands. *Water Resour. Res.* **1994**, *30*, 1241–1259.

41. Norman, J.; Kustas, W.; Humes, K. Source approach for estimating soil and vegetation energy fluxes in observations of directional radiometric surface temperature. *Agric. For. Meteorol.* **1996**, *77*, 263–293.

42. Bastiaanssen, W.G.M. Regionalization of surface flux densities and moisture indicators in composite terrain : A Remote Sensing Approach under Clear Sskies in Mediterranean Climates, Ph.D. Thesis, Wageningen University, Wageningen, The Netherlands, 1995.

43. Gowda, P.; Howell, T.; Paul, G.; Colaizzi, P.D.; Marek, T.H.; Su, B.; Copeland, K.S. Deriving hourly evapotranspiration rates with SEBS: A lysimetric evaluation. *Vadose Zo. J.* **2013**, *12(3)*, 1–11.

44. Hashem, A.A.; Engel, B.A.; Bralts, V.F.; Radwan, S.; Rashad, M. Performance evaluation and development of daily reference evapotranspiration model. *Irrig. Drain. Syst. Eng.* **2016**, *5*, 1–6.

45. Nash, J.E.; Sutcliffe, J. V. River flow forecasting through conceptual models part I - A discussion of principles. *J. Hydrol.* **1970**, *10*, 282–290.

46. Santhi, C.; Arnold, J.G.; Williams, J.R.; Dugas, W.A.; Srinivasan, R.; Hauck, L.M. Validation Of The SWAT Model On A Large Rwer Basin With Point And Nonpoint Sources. *J. Am. Water Resour. Assoc.* **2001**, *37*, 1169–1188.

47. Anderson, M.C.; Norman, J.M.; Mecikalski, J.R.; Torn, R.D.; Kustas, W.P.; Basara, J.B.; Anderson, M.C.; Norman, J.M.; Mecikalski, J.R.; Torn, R.D.; et al. A Multiscale Remote Sensing Model for Disaggregating Regional Fluxes to Micrometeorological Scales. *J. Hydrometeorol.* **2004**, *5*, 343–363.

48. Chávez, J.L.; Gowda, P.H.; Howell, T.A.; Copeland, K.S. Radiometric surface temperature calibration effects on satellite based evapotranspiration estimation. *Int. J. Remote Sens.* **2009**, *30*, 2337–2354.

49. Elhaddad, A.; Garcia, L.A.; Chávez, J.L. Using a Surface Energy Balance Model to Calculate Spatially Distributed Actual Evapotranspiration. *J. Irrig. Drain. Eng.* **2011**, *137*, 17–26.

50. Hashem, A.A.; Engel, B.A.; Rashad, M.; Ramadan, M.H.; Radwan, S.M. Development and validation of mathematical model for calculating daily reference evapotranspiration. In Proceedings of the American Society of Agricultural and Biological Engineers, Evapotranspiration: Challenges in Measurement & Modeling from Leaf to the Landscape Scale & Beyond, Raleigh, NC, USA, April 7–10, 2014.

51. Key, J.R.; Schweiger, A.J.; Stone, R.S. Expected uncertainty in satellite-derived estimates of the surface radiation budget at high latitudes. *J. Geophys. Res. C Ocean.* **1997**, *102*, 15837–15847.

52. Chávez, J.L.; Howell, T.A.; Copeland, K.S. Evaluating eddy covariance cotton ET measurements in an advective environment with large weighing lysimeters. *Irrig. Sci.* **2009**, *28*, 35–50.

53. Mkhwanazi, M.; Chávez, J.L.; Rambikur, E.H. Comparison of Large Aperture Scintillometer and Satellite-based Energy Balance Models in Sensible Heat Flux and Crop Evapotranspiration Determination. *Int. J. Remote Sens. Appl.* **2012**, *2*, 24.

54. Mkhwanazi, M.M.; Chávez, J.L. Mapping evapotranspiration with the remote sensing ET algorithms METRIC and SEBAL under advective and non-advective conditions: accuracy determination with weighing lysimeters. *Hydrol. Days* **2013**, *1*, 68–72.

55. French, A.N.; Hunsaker, D.J.; Thorp, K.R. Remote sensing of evapotranspiration over cotton using the TSEB and METRIC energy balance models. *Remote Sens. Environ.* **2015**, *158*, 281–294.

56. Long, D.; Singh, V.P. Assessing the impact of end-member selection on the accuracy of satellite-based spatial variability models for actual evapotranspiration estimation. *Water Resour. Res.* **2013**, *49*, 2601–2618.